ON THE CHOICE OF GEOMETRICAL IMPERFECTIONS IN GMNIA STRENGTH CALCULATIONS OF THIN-WALLED STRUCTURES

J. Kriváček[*], Z. Sadovský[**]

Abstract: *In the light of the recently developed method for implementation of initial geometrical imperfections in the ultimate buckling strength calculations of thin-walled structural elements by the materially and geometrically nonlinear FEM analysis (GMNIA), special choices of the imperfections are discussed.*

Keywords: Thin-walled structures, Geometrical imperfections, Strain energy, Ultimate strength, Non-linear finite-element simulations.

1. Introduction

A method for implementation of initial geometrical imperfections in the ultimate buckling strength calculations of thin-walled structural components has been developed in (Sadovský et al., 2012, Sadovský and Kriváček, 2017). The method takes into account imperfections in the shapes of eigenmodes of the corresponding linearized problem and their combinations. Essentially, any other imperfection shape, e.g. the measured shapes, can be used. Substantial feature of the method is that in the search for the most unfavourable shape the geometrical imperfections are normalized by the energy measure, i.e. imperfections are compared at an energy measure level. The energy measure EM of imperfections is defined by the square root of elastic strain energy of a structure hypothetically accumulated when the structure transfers from its presumed perfect state into the considered imperfect state. The energy measure is derived from the total strain energy (TSE) of the linear statics or linearized buckling FEM calculations. The applied commercial code MSC.Nastran (version 2013 and 2014) provides TSE as a by-product of the linearized buckling.

Some authors suggest that considering initial imperfections in the shapes of failure modes may lead to the most unfavourable ultimate strength values. In the present paper this conjecture is checked for the case of a cold formed lipped channel column in axial compression studied in (Sadovský and Kriváček, 2017).

The ultimate strengths are calculated using the load incremental arc-length approach of MSC.Nastran. Obtained results are compared with those of the MSC.Marc code (version 2016). Marc is executed from inside Nastran as MSC.Nastran Implicit Nonlinear solution (SOL 600, 106). For this solution a displacement incremental approach is applied.

2. Numerical study

Centreline cross-section dimensions, length and material properties of the channel are shown in Tab. 1. The cross-sectional dimensions and material properties correspond to the test specimen ST15A90 (Young and Hancock, 2003). The roundness of corners is not considered, thereby residual stresses are neglected and universal material model for cold-formed steel (von Mises yield criteria with isotropic hardening) is adopted. The task was carried out by the MSC.Nastran code applying the quadrilateral four-nodded linear QUAD4 element. Three element sizes of approximately 7.5, 5 and 3.3 mm have been used to produce meshes denoted as coarse, medium and fine, respectively. The multipoint constraint equations for element nodes located at the bottom end of the column ($x = 0$) provided uniform translation in axial direction. The
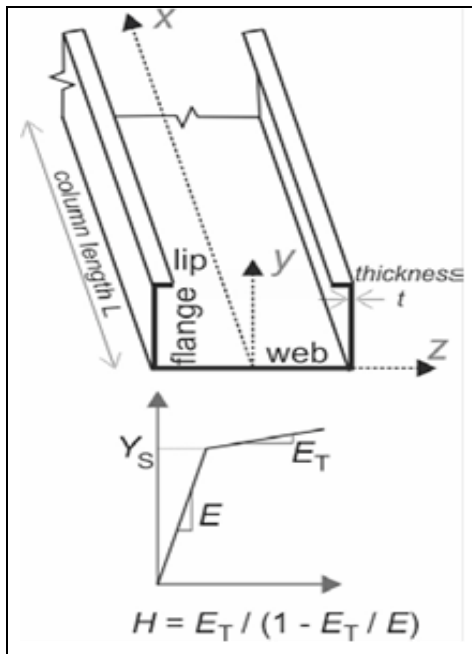
---

[*] Ing. Jozef Kriváček, CSc.: Institute of Construction and Architecture, Slovak Academy of Sciences, Dúbravská cesta 9; 845 03 Bratislava; SK, usarjkri@savba.sk

[**] Ing. Zoltán Sadovský, DrSc.: 831 03 Bratislava; SK, zoltan@sadovsky.info

translations in other directions and all translations of nodes at the column top end were fixed. These boundary conditions were chosen to match the attachment into the test rigs of the specimen ST15A90 (Young and Hancock, 2003) (see Sadovský et al., 2017).

Tab. 1: Dimensions and material characteristics of the studied channel.

web [mm]	97.4
flange [mm]	48
lip [mm]	9.95
thickness t [mm]	1.5
length L [mm]	2000
Young modulus E [GPa]	210
Poisson's ratio	0.3
yield stress Y_s [MPa]	515
plasticity modulus H [MPa]	21.002

$$H = E_T / (1 - E_T / E)$$

The presented results were obtained using the FEM model with medium mesh discretization (17 600 QUAD4 elements with 108 276 DOF).

The eigenmode imperfections — Modes 27, 28, 44 and the reversed Mode R27 (multiplying Mode 27 by -1) provided the least collapse loads among the first 60 eigenmodes normalized by the energy measure. (Sadovský et al., 2017). They are shown in Fig. 1 along with the chosen (moderate) energy measure level, the corresponding amplitudes and resulting failure loads. The term amplitude should be understood as the maximum of cross-sectional co-ordinate displacements.

Fig. 2 shows the corresponding failure shapes. For their use as initial imperfections the shapes are adjusted to the same energy measure level as given in Fig. 1. The corresponding amplitudes and failure loads obtained in subsequent calculations are presented in Fig. 2. Because the failure shapes are highly distorted, their normalisation by the energy measure resulted in significantly lower amplitudes than obtained for the eigenmodes. Note that only the cross-sectional displacements of the failure shapes are normalized and applied as initial imperfections. This corresponds to the measurements of initial out of nominal geometry of a member. Including the axial displacements would lead to even smaller amplitudes of the normalized shapes yielding higher values of failure loads.

The failure loads are defined as the peak of load-shortening response function of the channels. The function is obtained by load arc-length incremental solution. The channel is subject to axial load of 120 kN divided into ten uniform load steps. The magnitudes of individual load step increments were estimated by Crisfield type of arc-length method, so the increments could be less than zero. Stiffness update was performed at each iteration (full Newton-Raphson method) with error tolerance criteria of Load & Work (10^{-3}, 10^{-7}). The number of iterations for each increment was limited to 25. No convergence led to bisection of the increment and the solution was repeated. The number of controlled step increments was limited to 15. The problems with solution such as described in (Sadovský et al., 2017) did not occur in presented cases.

The MSC.Marc code with bilinear thin shell Element 139 is used to verify the failure loads given in Fig. 2. A displacement (shortening) incremental solution with Marc input data file generated by MSC.Nastran Implicit Nonlinear module (SOL 600, 106) (for details see Sadovský et al., 2017) is applied. Two uniform shortening steps (at $x = 0$) are adopted: 0.01 and 0.002 mm.
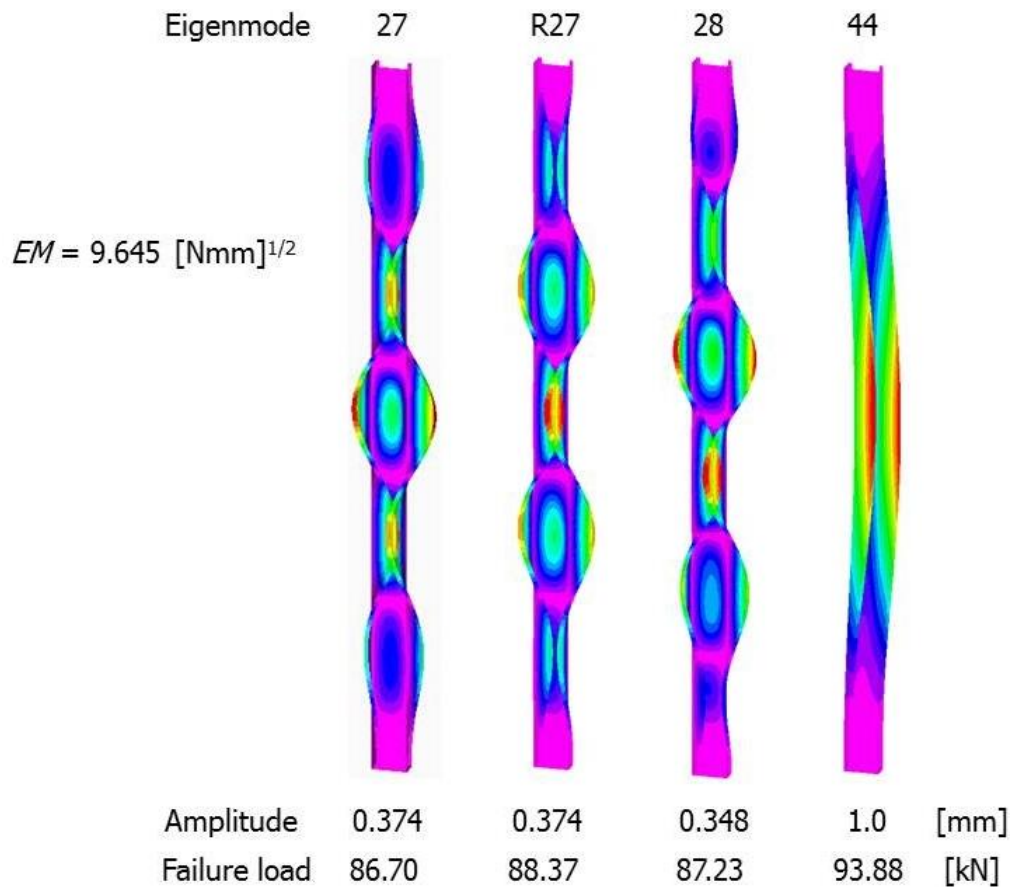
Fig. 1: The most influential eigenmode imperfections normalized to EM = 9.645 [N.mm]$^{1/2}$ with corresponding amplitudes and failure loads.

The Marc failure loads are given in Tab. 2. The largest difference occurred for R27 case. Solution of this case was recalculated using two ways: a) for load incremental arc-length solution smaller 5 kN load steps were applied and b) the shortening incremental solution by MSC.Nastran was adopted. The failure loads of 93.60 and 94.13 kN were obtained.

Tab. 2: Failure loads by MSC.Marc code.

Failure shape	27	R27	28	44
Failure load [kN]	100.82	97.12	100.26	103.89

Comparing the failure loads in Figs. 1 and 2 it is seen that in each individual eigenmode — failure shape succession of imperfections the latter provides markedly higher failure loads.

The CPU time consumption of load incremental solution ranged between 15 and 18 minutes. The displacement incremental solutions consumed larger amount of time – approximately 60 and 70 minutes for Marc and Nastran codes, respectively. Using ten times larger shortening increments decreased the time consumption to one sixth, however the value of failure load for Marc solution increased by 2.5 %. The change of Nastran strength value due to increase of shortening increments was negligible. Note that the calculations were performed on a work station with two eight-core Xeon processors (13 089 of cpu benchmark) and four SAS disks operating under Windows 7 ultimate.

The imperfections depicted in Fig. 2 were obtained as the sum of eigenmode imperfections given in Fig. 1 and the additional displacements at failure loads calculated for those imperfections (however without axial displacements as mentioned above). If applying only the additional displacements at failure loads as imperfections and normalizing them to $EM = 9.645$ [N.mm]$^{1/2}$, new amplitudes of 0.109, 0.163, 0.111 and 0.119 [mm] are obtained. Corresponding failure loads by MSC.Nastran arc-length approach are
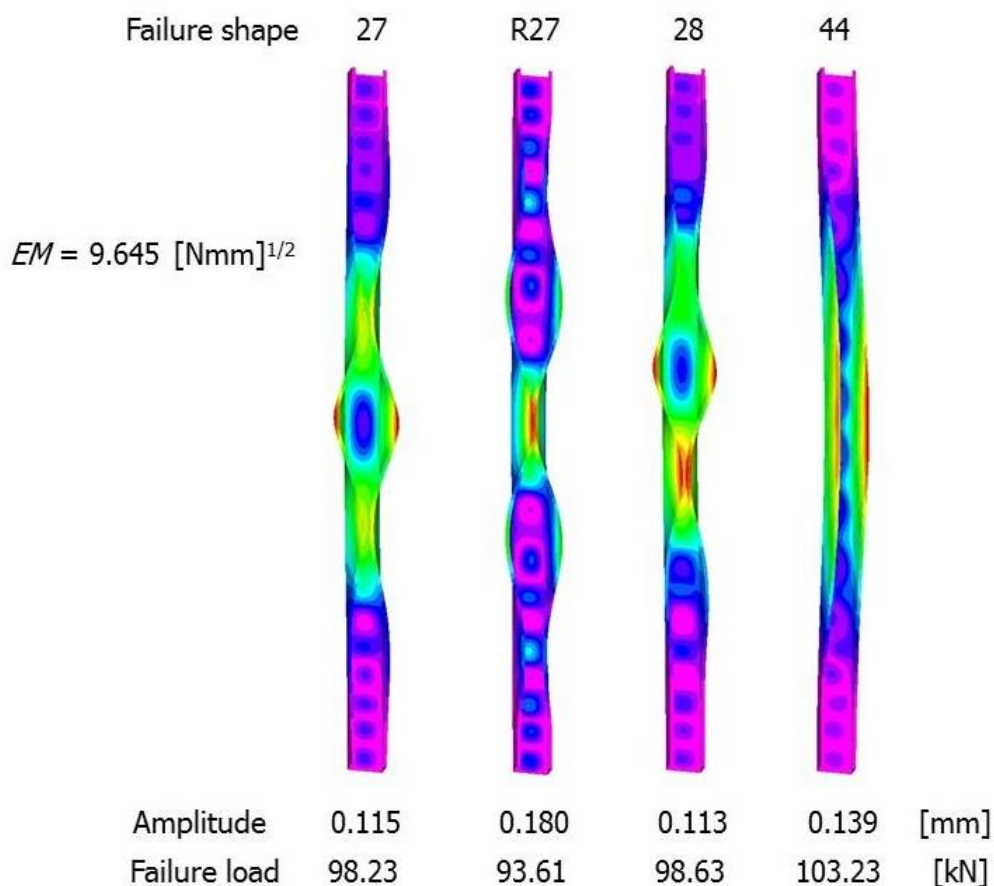
Fig. 2: The imperfections in failure shapes normalized to EM = 9.645 [N.mm]$^{1/2}$
with corresponding amplitudes and failure loads.

98.48 kN, 95.07 kN, 98.86 kN and 103.15 kN. These failure loads are also considerably higher than those in Fig. 1. Note that using only additional displacements at some load level as imperfections simplifies processing of input data for subsequent non-linear solution of this type of tasks.

3. Conclusions

Comparison of the most important eigenmode imperfections with the corresponding failure mode shapes revealed that under the energy measure normalization the latter possess significantly smaller amplitudes. This is a consequence of their high distortion, which suggests their classification as unrealistic imperfections. The corresponding failure loads are higher than those obtained for the eigenmode shapes normalized to the same energy measure level. For the eigenmode imperfection – Mode 27, providing the lowest failure load, the axial shortening at failure is about 7 % lower, while the maxima of lateral co-ordinate displacements at failure are 4.6 (z axis) and 2.7 (y axis) multiples of those obtained for the corresponding failure shape imperfection.

Acknowledgement

References

Sadovský, Z., Kriváček, J., Ivančo, V. and Ďuricová, A. (2012) Computational modelling of geometric imperfections and buckling strength of cold-formed steel. Journal of Constructional Steel Research, 78, pp. 1-7.

Sadovský, Z. and Kriváček, J. (2017) Tolerances of imperfections and strength of cold-formed lipped channel column. Journal of Constructional Steel Research, 128, pp. 762-771.

Young, B. and Hancock, G.J. (2003) Compression tests of channels with inclined simple edge stiffeners. Journal of Structural Engineering ASCE, 129, 10, pp. 1403-11.